Inorganic Chemistry

Article

pubs.acs.org/IC

A Series of Oxyimine-Based Macrocyclic Dinuclear Zinc(II) Complexes Enhances Phosphate Ester Hydrolysis, DNA Binding, DNA Hydrolysis, and Lactate Dehydrogenase Inhibition and Induces Apoptosis

Sellamuthu Anbu,[†] Subban Kamalraj,[‡] Babu Varghese,[⊥] Johnpaul Muthumary,[‡] and Muthusamy Kandaswamy*,[†]

[†]Department of Inorganic Chemistry, University of Madras, School of Chemical Sciences, Guindy Maraimalai Campus, Chennai 600 025, India

[‡]Centre for Advanced Study in Botany, University of Madras, Guindy Maraimalai Campus, Chennai 600 025, India

[⊥]Sophisticated Analytical Instruments Facility, Indian Institute of Technology, Chennai 600 036, India

Supporting Information

ABSTRACT: A symmetrical macrocyclic dizinc(II) complex (**1**) has been synthesized by using the ligand ($\mathbf{L^1}$) [μ-11,24-dimethyl-4,7,16,19-tetraoxa-3,8,15,20-tetraazatricyclo-[20.3.1.1^{10,13}] heptacosa-1(25),2,7,9,11,13(27),14,20,22(26),23-decaene-26,27-diol]. A series of unsymmetrical macrocyclic dizinc(II) complexes (**2**–**6**) has been synthesized by Schiff base condensation of bicompartmental mononuclear complex [**ZnL**] [μ-3,16-dimethyl-8,11-dioxa-7,12-diazadicyclo-[1.1^{14,18}] heptacosa-1,3,5(20),6,12,14,16,18(19)-octacaene-19,20-diolato)zinc(II)] with various diamines like 1,2-diamino ethane (L^2), 1,3-diamino propane (L^3), 1,4-diamino butane (L^4), 1,2-diamino benzene (L^5), and 1,8-diamino naphthalene (L^6). The ligand L^1 and all the zinc(II) complexes were structurally characterized. To corroborate the consequence of the aromatic moiety in comparison to the aliphatic moiety present in the macrocyclic ring on the phosphate ester hydrolysis, DNA binding and cleavage properties have been studied. The observed first order rate constant values for the hydrolysis of 4-nitrophenyl phosphate ester reaction are in the range from 2.73×10^{-2} to 9.86×10^{-2} s^{-1}.The interactions of complexes **1**–**6** with calf thymus DNA were studied by spectroscopic techniques, including absorption, fluorescence, and circular dichroism spectroscopy. The DNA binding constant values of the complexes were found in the range from 1.80×10^5 to 9.50×10^5 M^{-1}, and the binding affinities are in the following order: **6** > **5** > **1** > **2** > **3** > **4**. All the dizinc(II) complexes **1**–**6** effectively promoted the hydrolytic cleavage of plasmid pBR322 DNA under anaerobic and aerobic conditions. Kinetic data for DNA hydrolysis promoted by **6** under physiological conditions give the observed rate constant (k_{obs}) of 4.42 ± 0.2 h^{-1}, which shows a 10^8-fold rate acceleration over the uncatalyzed reaction of ds-DNA. The comparison of the dizinc(II) complexes **1**–**6** with the monozinc(II) complex [**ZnL**] indicates that the DNA cleavage acceleration promoted by **1**–**6** are due to the efficient cooperative catalysis of the two close proximate zinc(II) cation centers. The ligand $\mathbf{L^1}$, dizinc(II) complexes **1**, **3**, and **6** showed cytotoxicity in human hepatoma HepG2 cancer cells, giving IC_{50} values of 117, 37.1, 16.5, and 8.32 μM, respectively. The results demonstrated that **6**, a dizinc(II) complex with potent antiproliferative activity, is able to induce caspase-dependent apoptosis in human cancer cells. Cytotoxicity of the complexes was further confirmed by the lactate dehydrogenase enzyme level in HepG2 cell lysate and content media.

INTRODUCTION

Platinum(II) complexes are widely used and well-known metal-based drugs for cancer therapy,[1] but many of them possess inherent limitations such as side effects and resistance phenomena.[2] The non-platinum antitumor compounds can show various geometries and coordination numbers, various oxidation states, better solubility, feasible substitution kinetic pathways,[3a] and factors influencing the pharmacological profile different than those of platinum drugs.[3] Therefore, attempts are being made to replace these platinum-based drugs with suitable alternatives, and numerous metal complexes are synthesized and screened for their anticancer activities.[4,5] A wide repertoire of Zn^{II} complexes have been utilized as radioprotective agents,[6] tumor photosensitizers,[7] antidiabetic insulin-mimetic,[8] and antibacterial or antimicrobial agents.[9] It is also well-known that Zn^{II} is useful to reduce the cardio- and epatotoxicity induced by some anticancer drugs.[10] However, very little data on the cytotoxicity of zinc-based compounds against human cancer cell lines are as yet available.[11] Also, certain Zn^{II} complexes, which strongly bind and cleave DNA, exhibit prominent anticancer activities and regulate apoptosis.[12,13] However, these studies are mainly limited to mononuclear complexes, and very few studies on dinuclear complexes with

Received: November 14, 2011
Published: May 3, 2012

Zn^{II} ions in close proximity have been reported so far.[14] Recent studies have demonstrated that certain multinuclear Zn^{II} complexes can efficiently promote DNA cleavage by hydrolyzing the phosphate ester linkage.[14b] Sheng and co-workers have shown that the metal center is a crucial parameter in hydrolytic DNA cleavage, with the synergy between the metal ions contributing to the high nucleolytic efficiency of polynuclear Zn^{II} compounds.[14c] Therefore, designing new dinucleating ligands with different coordination entity having two Zn^{II} centers in close proximity is the great challenge in the rational nuclease synthesis. In light of this, many salient features of this metal, such as its ability to assist Lewis activation, nucleophile generation, leaving group stabilization, low toxicity, and its coordination states and geometries preserving the same oxidation state, induced us to investigate these newly synthesized dizinc(II) complexes as new potential anticancer agents. We have reported some of the side-off, macrobicyclic, macrocyclic dinuclear oxovanadyl(II), copper(II) and nickel(II) complexes, which avidly bind and efficiently cleave DNA under physiological conditions.[15] Very recently, we have found that the bis-phenanthroline water bridged dicopper(II) complex plays a pivotal role in the DNA hydrolysis and mechanism underlying induction of cell death.[16] Encouraged by the results obtained in the DNA binding and cleavage experiments for oxyimine-based macrocyclic dicopper(II) and dinickel(II) complexes, we decided to evaluate the effect of dizinc(II) analogues toward nucleic acid degradation and cytotoxic activity in vitro against the human hepatoma HepG2 cancer cell lines. In this context, here we report synthesis, characterization of a oxyimine based symmetrical and a series of unsymmetrical macrocyclic dinuclear complexes involving Zn^{II} ion (Scheme 1) in two different coordination environments and their phosphate ester hydrolysis, DNA binding, DNA hydrolysis, and anticancer properties.

EXPERIMENTAL SECTION

Materials and Methods. 2,6-Diformyl-4-methylphenol[17] and 1,2-bis(aminooxy)ethane[18] were prepared from the literature methods. Zinc(II) perchlorate hexahydrate (Aldrich), calf thymus CT−DNA (highly polymerized stored at 4 °C), superoxide dismutase (SOD), pBR322 supercoiled plasmid DNA, ethidium bromide (EB), and agarose (Genei, Bangalore, India) were used as received. Ultrapure Milli-Q water (18.2 mΩ) was used in all experiments. All other chemicals and solvents were of analytical grade and used as received, without any further purification.

Scheme 1. Synthesis of Macrocyclic Dizinc(II) Complexes 1−6

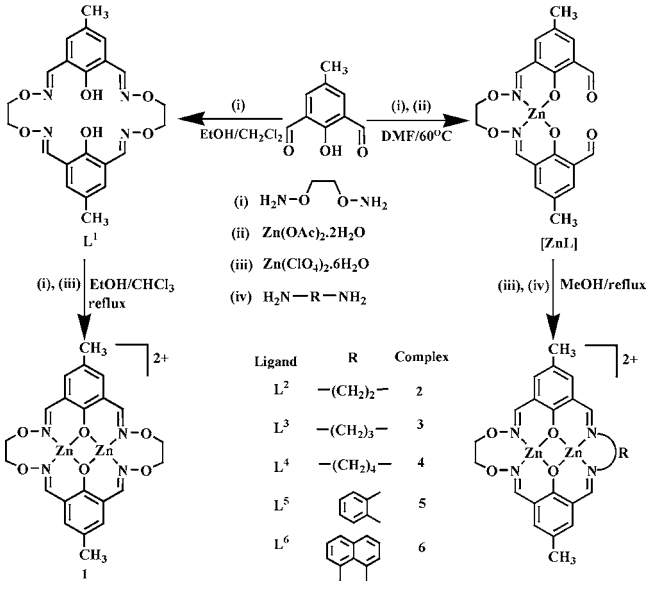

Elemental analysis was carried out on a Carlo Erba model 1106 elemental analyzer. Fourier transform infrared (FTIR) spectra were obtained on a Perkin-Elmer FTIR spectrometer with sample prepared as KBr pellets. UV−visible spectra were recorded using a Perkin-Elmer Lambda 35 spectrophotometer operating in the range of 200−1100 nm with quartz cells and ε are given in M^{-1} cm^{-1}. NMR spectra were recorded in $CDCl_3$ and DMSO-d_6 by using TMS as an internal standard on a BRUKER 400 MHz spectrometer. ESI mass spectral measurement was carried out using a Thermo Finnigan LCQ-6000 Advantage Max-ESI mass spectrometer. Solutions of DNA in 5 mM Tris-HCl/50 mM NaCl (pH = 7.1) buffer gave the ratio of UV absorbance at 260 and 280 nm, A_{260}/A_{280}, of 1.9, indicating that the DNA was sufficiently free of protein.[19] Concentrated stock solutions of DNA (10.5 mM) were prepared in a 5 mM Tris−HCl/50 mM NaCl buffer and sonicated for 25 cycles, where each cycle consisted of 30 s with 1 min intervals. The concentration of DNA in nucleotide phosphate (NP) was determined by UV absorbance at 260 nm after 1:100 dilutions. The extinction coefficient, ε_{260}, was taken as 6600 M^{-1} cm^{-1}. Stock solutions were stored at 4 °C and used after no more than 4 days. Supercoiled plasmid pBR322 DNA was stored at −20 °C and the concentration of DNA in base pairs was determined by UV absorbance at 260 nm after appropriate dilutions taking ε_{260} as 13 100 M^{-1} cm^{-1}. Concentrated stock solutions of metal complexes were prepared by dissolving calculated amounts of zinc(II) complexes in a 2.5% DMF/5 mM Tris−HCl/50 mM NaCl buffer to required concentrations for all experiments.

Synthesis of Macrocyclic Dinucleating Ligand (L^1). 2,6-Diformyl-4-methyl phenol (3.0 g, 182 mmol) in dichloromethane (100 mL) and 1,2-bis(aminooxy)ethane (1.68 g, 182 mmol) in absolute ethanol were added simultaneously over a period of 6 h to a mixture of dichloromethane (300 mL) and ethanol (100 mL). After complete addition, the reaction mixture was stirred at 25 °C for 12 h. The solvent was then removed at reduced pressure and the resulting colorless suspension was evaporated to dryness. The colorless crystals suitable for X-ray diffraction (XRD) analysis were obtained by slow evaporation of dichloromethane and methanol mixture. Yield: 3.8 g (81%); white solid; mp 173 °C. IR (KBr, cm^{-1}): 3416 (ν O−H) (br), 2929 ν(C−H) (s), 1617 ν(C═N) (s), 1074 ν (O−C) (s). ^{1}H NMR (400 MHz, $CDCl_3$): 2.27 (CH_3, s, 6H), 3.78 (O−CH_2−, d, 8H ; J = 6.2 Hz), 7.26 (ArH, s, 4H), 8.38 (CH═N, s, 4H), 9.54 (Ar−OH, s, 2H). ^{13}C NMR ($CDCl_3$, 100 MHz): 20.29 (CH_3), 72.84 (CH_2), 118.29, 128.85, 130.7, 131.52, and 155.8 (Ar−C), δ 166.18 (Ar−CH). Anal. Calcd for $C_{22}H_{24}N_4O_6$: C, 59.99; H, 5.50; N, 12.70%. Found: C, 59.58; H, 5.20; N, 12.10%. ESI−MS in CH_3OH: (m/z) 441.21 $[M + H]^+$.

Synthesis of Macrocyclic Dinuclear Zinc(II) Complexes. Caution! *Although no problems were encountered in this work, transition metal perchlorate complexes are potentially explosive and should be handled with proper precautions.*[20]

Synthesis of $[Zn_4(L^1)_2(\mu\text{-}OH)_2](ClO_4)_2$ (1). An ethanolic solution of zinc(II) perchlorate hexahydrate (0.169 g, 0.45 mmol) (10 mL) was added to the hot solution of macrocyclic ligand L^1 (0.1 g, 0.23 mmol) in ethanol and chloroform mixture (20 mL) (1: 1, v/v). The mixture was refluxed for 6 h. The resulting pale yellow solution was then filtered in hot condition and allowed to stand at room temperature. After slow evaporation of the solvent at 25 °C, the pale yellow compound was obtained, washed with cold ethanol, and dried in a vacuum. Pale yellow crystals suitable for X-ray analysis were obtained after two weeks by slow evaporation of an ethanol solution. Yield: 0.12 g (77%); Pale yellow solid; IR (KBr, cm^{-1}): 3450 ν(OH) (br),1635 ν(C═N) (s), 1110 (vs) $\nu(ClO_4^-)$, 625 (s) $\nu(ClO_4^-)$. λ_{max}, nm (ε, M^{-1} cm^{-1}) in CH_3CN: 248 (185,000), 310 (18900). ^{1}H NMR (400 MHz, DMSO-d_6): 2.21(CH_3, s, 6H), 4.22 (O−CH_2−, d, 8H ; J = 6.8 Hz), 7.32 (ArH, s, 4H), 8.42 (CH═N, s, 4H). Anal. Calcd for

dx.doi.org/10.1021/ic202451e | Inorg. Chem. 2012, 51, 5580−5592

$C_{44}H_{46}Cl_2N_8O_{22}Zn_4$: C, 38.54; H, 3.38; N, 8.17; Zn, 19.07%. Found: C, 38.41; H, 3.31; N, 8.09; Zn, 19.12%. ESI−MS in CH_3OH: (m/z) 600 $[Zn_2L^1(H_2O)(OH)\text{-}ClO_4]^+$.

Synthesis of Dinucleating Bicompartmental Mononuclear Complex (ZnL). To a solution of 2,6-diformyl-4-methyl phenol (3.0 g ; 18 mmol) in warm dimethyl formamide (15 mL), 1,2-bis(aminooxy)-ethane (0.84 g. 0.9 mmol) was added dropwise under constant stirring. Then the solid $Zn(OAc)_2{\cdot}2H_2O$ (2.0 g ; 0.9 mmol) was added and the solution was stirred at 60 °C for 2 h. The resulting mononuclear complex [**ZnL**] precipitated. The yellow solid was separated by vacuum filtration and washed with 2-propanol and diethyl ether. Yield: 3.20 g (55%); Yellow solid; IR (KBr, cm^{-1}): 3425 ν(OH) (br), 2923 ν(C−H) (s),1680 ν(C═O) (s), 1634 ν(C═N) (s). $\lambda_{max,}$ nm (ε, M^{-1} cm^{-1}) in DMF: 228 (165,000), 257 (16600). ^{1}H NMR (400 MHz, DMSO-d_6): 2.24 (CH_3, s, 6H), 3.98 (O−CH_2−, s, 4H), 7.31 (ArH, s, 2H), 7.68 (ArH, s, 2H), 8.42 (CH═N, s, 2H), 10.52 (CH═O, s, 2H). Anal. Calcd for $C_{20}H_{18}N_2O_6Zn$: C, 53.65; H, 4.05; N, 6.26; Zn, 14.60%. Found: C, 53.49; H, 3.97; N, 6.19; Zn, 14.53%.

Synthesis of $[Zn_2L^2(H_2O)_2](ClO_4)_2(H_2O)_3$ (2). The dinuclear Zn^{II} complex **2** was prepared from a general synthetic procedure in which the vigorously stirred suspension of mononuclear complex **ZnL** (0.25 g, 0.57 mmol) in methanol (25 mL), a methanolic solution of $Zn(ClO_4)_2{\cdot}6H_2O$ (0.2 g, 0.57 mmol) was added slowly and the mixture was stirred for 15 min to obtain a clear solution. Then the methanolic solution (5 mL) of 1,2-diamino ethane (0.035 g; 0.57 mmol) was added dropwise to the above solution and refluxed for 3 h. A pale yellow solid was separated on evaporating the solution at room temperature and the resulting compound was washed with ether and dried. Recrystallization from acetonitrile solution offered greenish yellow solid. Yield: 0.33 g (77%); yellow solid; IR (KBr, cm^{-1}): 3434 ν(OH) (br), 2921 (C−H) (s),1625 (C═N) (s), 1089 (vs) $\nu(ClO_4^-)$, 623 (m) $\nu(ClO_4^-)$. $\lambda_{max,}$ nm (ε, M^{-1} cm^{-1}) in CH_3CN: 235 (192,000), 280 (19500). ^{1}H NMR (400 MHz, DMSO-d_6): 2.22 (CH_3, s, 6H), 3.76 (N−CH_2, s, 4H),4.16 (O−CH_2−,s, 4H), 7.12 (ArH, s, 2H), 7.45 (ArH, s, 2H), 8.48 (CH═N, s, 2H), 8.62 (CH═N, s, 2H). Anal. Calcd for $C_{22}H_{26}Cl_2N_4O_{14}Zn_2$: C, 34.22; H, 3.39; N, 7.26; Zn, 16.94%. Found: C, 34.16; H, 3.24; N, 7.19; Zn, 16.76%. ESI−MS in CH_3OH: (m/z) 284, $[Zn_2L^2-2ClO_4]^{2+}$.

Synthesis of $[Zn_2L^3(H_2O)_2](ClO_4)_2(H_2O)_3$ (3). This complex was prepared by the method used for **2**, using 1,3-diamino propane (0.04 g; 0.57 mmol) in place of 1,2-diamino ethane, offered pale yellow solid. Yellow crystals suitable for X-ray analysis were obtained after two weeks by slow evaporation of acetonitrile solution. Yield: 0.35 g (81%); yellow solid; IR (KBr, cm^{-1}): 3439 ν(OH) (br), 2923 (C−H) (s),1631 (C═N) (s), 1092 (vs) $\nu(ClO_4^-)$, 625 (m) $\nu(ClO_4^-)$. $\lambda_{max,}$ nm (ε, M^{-1} cm^{-1}) in CH_3CN: 239 (194,000), 285 (19,200). ^{1}H NMR (400 MHz, DMSO-d_6): 2.03, (−CH_2−, m, 2H ; J = 6.6 Hz), 2.18 (CH_3, s, 6H), 3.26 (N−CH_2, t, 4H ; J = 6.8 Hz), 4.18 (O−CH_2−, s, 4H), 7.09 (ArH, s, 2H), 7.52 (ArH, s, 2H), 8.42 (CH═N, s, 2H), 8.72 (CH═N, s, 2H). Anal. Calcd for $C_{23}H_{34}Cl_2N_4O_{17}Zn_2$: C, 32.88; H, 4.08; N, 6.67; Zn, 15.56%. Found: C, 32.96; H, 4.15; N, 6.76; Zn, 15.42%. ESI−MS in CH_3CN: (m/z) 291, $[Zn_2L^3-2ClO_4]^{2+}$.

Synthesis of $[Zn_2L^4(H_2O)_2](ClO_4)_2$ (4). This complex was prepared by the method used for **2**, using 1,4-diamino butane (0.05 g; 0.57 mmol) in place of 1,2-diamino ethane, offered pale yellow solid. Yield: 0.36 g (80%); yellow solid; IR (KBr, cm^{-1}): 3441 ν(OH) (br), 2923 (C−H) (s),1624 (C═N) (s), 1095(vs) $\nu(ClO_4^-)$, 626 (m) $\nu(ClO_4^-)$. $\lambda_{max,}$ nm (ε, M^{-1} cm^{-1}) in CH_3CN: 242 (197,000), 290 (19,000). ^{1}H NMR (400 MHz, DMSO-d_6): 1.54, (CH_2, m, 4H; J = 6.8 Hz), 2.08 (CH_3, s, 6H), 3.44, (CH_2, t, 4H; J = 6.6 Hz), 4.23 (O−CH_2−, s, 4H), 7.46 (ArH, s, 2H), 7.51 (ArH, s, 2H), 8.15 (CH═N, s, 2H), 8.36 (CH═N, s, 2H). Anal. Calcd for $C_{24}H_{30}Cl_2N_4O_{14}Zn_2$: C, 36.02; H, 3.78; N, 7.00; Zn, 16.34%. Found: C, 35.92; H, 3.62; N, 6.91; Zn, 16.04%. ESI−MS in CH_3OH: (m/z) 298, $[Zn_2L^4-2ClO_4]^{2+}$.

Synthesis of $[Zn_2L^5(H_2O)_2](ClO_4)_2$ (5). This complex was prepared by the method used for **2**, using 1,2-diamino benzene (0.06 g; 0.57 mmol) in place of 1,2-diamino ethane, offered yellow solid. Yield: 0.38 g (82%); yellow solid; IR (KBr, cm^{-1}): 3445 ν(OH) (br), 1638 (C═N) (s), 1097 (vs) $\nu(ClO_4^-)$, 624 (m) $\nu(ClO_4^-)$. $\lambda_{max,}$ nm (ε, M^{-1} cm^{-1}) in CH_3CN: 280 (170,000), 305 (79,000). ^{1}H NMR (400 MHz, DMSO-d_6): 2.15 (CH_3, s, 6H), 4.28 (O−CH_2−, s, 4H), 6.35 (ArH, dd, 4H; J = 6.8 Hz), 6.48 (ArH, s, 2H), 6.55 (ArH, d, 4H; J = 6.8 Hz), 7.16 (ArH, s, 2H), 8.12 (CH═N, s, 2H), 8.54 (CH═N, s, 2H). Anal. Calcd for $C_{26}H_{26}Cl_2N_4O_{14}Zn_2$: C, 38.07; H, 3.20; N, 6.83; Zn, 15.95%. Found: C, 37.91; H, 3.14; N, 6.76; Zn, 15.65%. ESI−MS in CH_3OH: (m/z) 308, $[Zn_2L^5-2ClO_4]^{2+}$.

Synthesis of $[Zn_2L^6(H_2O)_2](ClO_4)_2$ (6). This complex was prepared by the method used for **2**, using 1,8-diamino naphthalene (0.085 g; 0.57 mmol) in place of 1,2-diamino ethane, offered yellow solid. Yield: 0.36 g (75%); yellow solid; IR (KBr, cm^{-1}): 3440 ν(OH) (br), 1637 (C═N) (s), 1098 (vs) $\nu(ClO_4^-)$, 625 (m) $\nu(ClO_4^-)$. $\lambda_{max,}$ nm (ε, M^{-1} cm^{-1}) in CH_3CN: 285 (175,000), 310 (87,000). ^{1}H NMR (400 MHz, DMSO-d_6): 2.07 (CH_3, s, 6H), 4.28 (O−CH_2, s, 8H), 7.28 (N−CH_2, d, 2H ; J = 7.2 Hz), 7.44 (Ar−H, dd, 2H; J = 7.4 Hz), 7.74 (Ar−H, t, 2H; J = 6.8 Hz), 8.38 (CH═N, s, 2H), 8.61 (CH═N, s, 2H). Anal. Calcd for $C_{30}H_{28}Cl_2N_4O_{14}Zn_2$: C, 41.40; H, 3.24; N, 6.44; Zn, 15.03%. Found: C, 41.24; H, 3.09; N, 6.25, Zn, 14.93%. ESI−MS in CH_3OH: (m/z) 333, $[Zn_2L^6-2ClO_4]^{2+}$.

Phosphate Ester Hydrolysis. The hydrolysis of 4-nitrophenyl phosphate (4-NPP) ester was run on the UV spectrophotometer following the increase in absorption at 400 nm due to d[4-NPP]/dt. The effect of pH on the reaction rate for the hydrolysis of 4-NPP ester promoted by complexes **1**−**6** was determined over the pH range 3.9−10.5. Reactions were performed using the following conditions: 3000 μL of freshly prepared buffer aqueous solution (50 mM, 0.1 mM $NaClO_4$, buffer: acetato (pH 3.9−5.2), MES (pH 5.8−6.5), bis-Tris propano (pH 7.2−8.5), CHES (pH 8.98−10.50), and 1000 μL of complex solution (5.00×10^{-4} M [acetonitrile−water (2.5% (v/v))]) were added to a 1 cm path length at 25 °C. The reaction was initiated with the addition of 100 μL of an acetonitrile substrate solution (4-NPP) (5.00×10^{-5} M). The reactions were corrected for the degree of ionization of the 4-nitrophenol at the respective pH and temperature using the molar extinction coefficients for 4-nitrophenolate at 400 nm.[21] Reactions were monitored to less than 5% conversion of the substrate, and the data were treated using the initial rate method. The pseudo-first-order rate constants k_{obs} (s^{-1}) were calculated from the slope of the linear plot of $\ln(A_\infty - A_t)$ versus time. Under conditions of excess substrate, correction for the spontaneous hydrolysis of the phosphate ester was accomplished by direct difference using a reference cell in identical conditions without adding the catalyst. In the case of excess complex the reaction rates were uncorrected for spontaneous hydrolysis. For slow reactions (pH < 6.5) absorbance data were collected over one half-life and the final value of A_∞ was obtained after 4 days at 25 °C. Above pH 6.5, absorbance data were collected for up to three half-lives. The quoted rate constants are the average of duplicate runs.

Cytotoxicity Studies. Human hepatoma HepG2 cancer cell line was obtained from National Centre for Cell Science (NCCS), Pune, India, and cell viability was assessed by the MTT (3,4,5-dimethylthiazolyl-2-2,5-diphenyltetrazolium bromide) method. HepG2 cells were maintained in a humidified atmosphere containing 5% CO_2 at 37 °C in DMEM medium supplemented with 100 units of penicillin, 100 μg/mL of streptomycin, and 10% fetal bovine serum. Briefly, HepG2 cells with a density 1×10^4 cells per well were precultured in 96-well microtiter plates for 48 h under 5% CO_2. The ligand L^1, $Zn(ClO_4)_2{\cdot}6H_2O$, **1**, **3**, and **6** were added in microwells containing the cell culture at the concentration of 2−100 μM. Then each well was loaded 10 μL MTT solution (5 mg mL^{-1} in PBS pH = 7.4) for 4 h at 37 °C. The insoluble formazan was dissolved in 100 μL of 4% DMSO and the cell viability was determined by measuring the absorbance of each well at 570 nm using Bio-Rad 680 microplate reader (Bio-Rad, USA). All experiments were performed in triplicate and the percentage of cell viability was calculated according to the following equation. After 48 h, the cells were observed with an inverted phase contrast microscope, photographed with a Nikon FM 10 camera.

dx.doi.org/10.1021/ic202451e | Inorg. Chem. 2012, 51, 5580−5592

Table 1. Crystallographic Data for L^1, Zn^{II} Complexes 1 and 3

parameters	L^1	complex 1	complex 3
empirical formula	$C_{22}H_{24}N_4O_6$	$C_{44}H_{46}Cl_2N_8O_{22}Zn_4$	$C_{23}H_{24}Cl_2N_3O_{12}Zn_2$
formula weight	440.45	1371.27	830.14
T (K)	293(2)	293(2)	293(2)
wavelength (Å)	0.71073	0.71073	0.71073
crystal system	triclinic	monoclinic	orthorhombic
space group	$P\bar{1}$	$C2/c$	$Pca21$
a (Å)	8.0437(4)	18.6996(7)	26.1009(14)
b (Å)	11.2976(5)	24.5936(9)	8.0055(4)
c (Å)	12.0851(5)	16.0255(9)	16.6468(8)
α (°)	99.996(1)	90	90
β (°)	94.296(1)	123.870(2)	90
γ (°)	101.084(1)	90	90
volume A^3	1054.70(8)	6119.3(5)	3478.4(3)
Z	2	4	5
calc density Mg/m^3	1.387	1.488	1.757
abs coefficient mm^{-1}	0.103	1.713	1.984
crystal size (mm)	0.25 × 0.15 × 0.15	0.3 × 0.2 × 0.2	0.3 × 0.2 × 0.2
θ range for data collection (°)	1.72−28.27	1.58−23.75	1.56−25.42
max and min transmission	0.982 and 0.985	0.6275 and 0.7257	0.627 and 0.726
data/restraints/parameters	5199/0/291	4656/6/365	5916/1/433
final R indices $[I > 2\sigma(I)]$	R_1 = 0.0412	R_1 = 0.0608	R_1 = 0.0745
R indices (all data)	wR_2 = 0.1391	wR_2 = 0.1735	wR_2 = 0.2196
largest diff peak and hole $e{\cdot}A^{-3}$	0.250 and −0.180	2.480 and −1.170	0.813 and −0.773

$$\text{inhibition rate (IR\%)} = \frac{\text{OD (control)} - \text{OD drug treated cells}}{\text{OD (control)}} \times 100\% \quad (2)$$

Annexin V-FITC Conjugate Staining for HePG2. After 48 h, IC_{50} concentrations of $Zn(ClO_4)_2{\cdot}6H_2O$, L^1, **1**, **3**, and **6** treated and controlled cells were washed twice with 1× PBS buffer and stained with Annexin V-FITC conjugate (200 μL of Annexin V-FITC and 1.8 mL of 1× binding buffer) in a four-well Labtek II chambered cells for 15 min and images observed under the microscope. The appropriate amount of binding buffer added should be sufficient to ensure that the slide must not dry out during fluorescence microscopic observation. The cells were examined by using Neofluar 40× lens and then photographed as described above.

Analysis of Cell Cycle Progression. Cells were seeded in 25 cm^2 flask at the density of 1 × 10^6 cells/flask. After 24 h, IC_{50} concentrations of L^1, **1**, **3**, and **6** were added to the respective flasks and incubated for 48 h. Cells were trypsinized, harvested, and fixed in 5 mL of 80% cold ethanol in test tubes and incubated at 4 °C for 15 min. After incubation, the cells were centrifuged at 1500 rpm for 5 min and the cell pellets were resuspended in 500 μL of propidium iodide (PI) (10 μg/mL) containing 300 μg/mL RNAase (Sigma, Chennai). Then cells were incubated on ice for 30 min and filtered through 53 μm nylon mesh. Cell cycle distribution was analyzed by using FACS can (Becton-Dickinson) with 15 mw, 488 nm argon ion laser. PI signals were collected using 585/42 band-pass filter. The data acquired were analyzed with cell quest software.

Western Blot Analysis. Whole cellular proteins were extracted by incubation the cell pellets with cell lysis buffer (Cell Signaling Technology) overnight at 4 °C. Protein concentration was determined by the bicinchoninic acid assay (Sigma, Chennai) according to the manufacturer's instructions. SDS−PAGE was done in 10% tricine gels loading 40 mg of cell lysates per lane. After electrophoresis, separated proteins were transferred to nitrocellulose membrane and blocked with 5% nonfat milk in TBST buffer for 1 h. After that, the membranes were incubated with primary antibodies at 1:1000 dilutions in 5% nonfat milk overnight at 4 °C with continuous agitation, and then secondary antibodies were conjugated with horseradish peroxidase at 1:2000 dilution for 1 h at room temperature. Protein bands were visualized on X-ray film using an enhanced chemiluminescence system (Kodak). All the blots were stripped and reprobed with polyclonal anti-β-actin antibody to ascertain equal loading of proteins.

Assay of Lactate Dehydrogenase (LDH). Glycine buffer (0.1 M) (pH 7.4), buffered substrate (lithium lactate in NaOH), NAD^+ (5 mg/mL), 0.02% dinitro phenyl hydrazine (DNPH) in 1 N HCl, 0.4 N NaOH and stock standard trisodium pyruvate were purchased from Genei India. LDH assay was measured in both cell lysate and in the conditioned medium. After 48 h incubation, the culture medium with treatment was taken separately and the attached cells were lysed by adding 0.1% Triton X100 and subjecting them to two cycles of freezing and thawing. The activity of LDH was measured by following King's method.[22] The substrate reaction buffer containing 0.5 mM lactic acid, 0.1 N NaOH, and 0.1 M glycine buffer was added to the cell lysate and medium and then 0.02 mL of NAD was added to both. DNPH (0.02%) was added as chromogenic agent and the absorbance values at 460 nm were read in UV spectrophotometer. The units were expressed in μM of pyruvate liberated/min/mg of protein.

$$\%\text{of leakage of LDH} = \frac{\text{activity in medium}}{\text{activity in cells} + \text{activity in medium}} \times 100 \quad (3)$$

RESULT AND DISCUSSION

Syntheses and Structural Analyses of Complexes. The present work stems from our interest in designing new symmetrical and unsymmetrical macrocyclic ligands and their dinuclear zinc(II) complexes. In symmetrical dizinc(II) complex, both zinc(II) ions are in oxyimine compartments, whereas the unsymmetrical dizinc(II) analogues, one compartment of the unsymmetrical macrocyclic ligand size is fixed by oxyimine moiety and other side of the macrocyclic ring size is modified by condensing various alkyl and aromatic diamines. All of the complexes have been obtained in good yield. The crystal structures of L^1, **1**, and **3** have been determined by using single crystal X-ray diffraction analysis, and they are consistent with the proposed formula of the complexes. The selected crystallographic data of L^1, **1**, and **3** are given in Table 1. The related unsymmetrical dizinc(II) complexes **4**−**6** are suggested

dx.doi.org/10.1021/ic202451e | Inorg. Chem. 2012, 51, 5580−5592

that they have similar structures, which is supported by ^{1}H−NMR and ESI−MS data (Figures S1−S8 in the Supporting Information). All the complexes **1**−**6** are soluble in a 2.5% DMF/5 mM Tris−HCl/50 mM NaCl buffer at pH 7.0, and they exhibit two intense bands in the UV region (240−300 nm) attributed to the intraligand $\pi-\pi^*$ transitions within the coordinated phenolate moiety and imines. There was no band observed in the visible region. In the ^{1}H NMR spectrum of ligand $\mathbf{L^1}$, singlets of methylene protons and oxime protons were observed at 3.8 and 8.5 ppm, respectively, showing the symmetrical structure of macrocyclic ligand $\mathbf{L^1}$. The OH resonance at 9.6 ppm strongly suggests intramolecular hydrogen bonds between the oxime nitrogen and the phenolic hydroxyl groups. This is consistent with the crystal structure of the macrocyclic ligand $\mathbf{L^1}$. In the ^{13}C NMR spectra of $\mathbf{L^1}$, the signals of the C═N carbon atoms were observed at 164 ppm. The IR spectrum clearly indicates the C═N group, because C═N stretching absorption band of the ligand was observed at 1617 cm^{-1}. A very strong and broad band near 1100 cm^{-1} and a strong and sharp band near 625 cm^{-1} are observed in the IR spectra of the dizinc(II) complexes **1**−**6**, which could be due to the antisymmetric stretching and bending of perchlorate ions, respectively. No splitting pattern of perchlorate peak was observed. This indicates that the perchlorate ions were not coordinated to the Zn^{II} ions and present as counterions in the crystal lattice. The ESI mass spectrum of a ligand $\mathbf{L^1}$ exhibited intense peak at m/z = 441.73 (calcd. m/z = 440.13) which has been assigned to the $[L^1 + H]^+$ ion. No peak from the mononuclear zinc(II) complex [ZnL] was detected, since it is electrically neutral. The complex **1** showed peaks at m/z = 1264.27, 600.39, 582.37, and 291.07 that corresponds to $[Zn_4(L^1)_2)(OH)_2(ClO_4)-ClO_4]^+$, $[Zn_2L^1(H_2O)(OH)-ClO_4]^+$, $[Zn_4L^1(OH)_2-2ClO_4]^{2+}$, and $[Zn_2L^1(H_2O)-(OH)-(ClO_4)]^{2+}$, respectively. The complexes **2**−**6** showed peaks at 284.20, 291.27, 298.11, 308.20, and 333.21, which have been assigned to $[Zn_2L^{2-6}-2ClO_4]^{2+}$, respectively. This is consistent with the exclusive formation of $[Zn_2L^{2-6}-2ClO_4]^{2+}$ observed in the ^{1}H NMR and elemental analysis. In the ^{1}H NMR spectrum of mononuclear zinc(II) complex [**ZnL**], a singlet observed around at δ = 10.6 ppm is due to aldehydic protons, which is absent in all the unsymmetrical complexes (**2**−**6**) and thus indicate the formation of Schiff base unsymmetrical macrocyclic ligands $\mathbf{L^2}$−$\mathbf{L^6}$. The structure of the dinuclear complex **3** in solution is essentially the same as that in the crystalline state because the nonequivalent ^{1}H NMR spectral pattern is consistent with the unsymmetrical feature found in the crystalline state. The OCH_2-CH_2O protons of symmetrical macrocyclic ligand $\mathbf{L^1}$ showed a singlet at δ = 3.78 ppm. Significant downfield shift of the peak corresponding to OCH_2-CH_2O protons in ligands (L^{1-6}) from 3.78 to 4.28 ppm upon addition of Zn^{II} ions clearly indicate the metal coordination of oxyimine nitrogen atoms.

Description of Crystal Structure of $\mathbf{L^1}$. The symmetrical macrocyclic dinucleating ligand $\mathbf{L^1}$ (Figure 1) crystallizes in the triclinic system with space group $P\bar{1}$ and two halves of the molecules in the asymmetric unit. The asymmetric unit joins to its centrosymmetric equivalent to form the complete macrocyclic ligand. The two CH_2 group carbons (C21 and C22) do not belong to the asymmetric unit. The molecules and their c-translational equivalents are linked through CH···O hydrogen bonding interaction (C18 H18···O2 ($-x$, $-y$, 2 − z)) (0.93 Å, 2.53 Å and 163.8°), (C8 H8···O6 (1 − x, $-y$, 1 − z)) (0.93 Å, 2.59 Å and 151.92°). The packing is further stabilized through van der Waals interactions (Figure S9 in the Supporting Information).

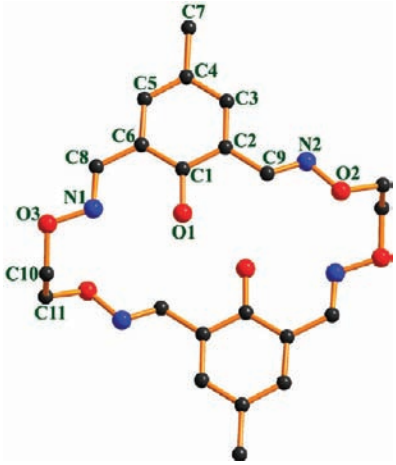

Figure 1. Crystal structure of symmetrical macrocyclic ligand $\mathbf{L^1}$. Hydrogen atoms are omitted for the sake of clarity.

Description of Crystal Structure of $[Zn_4(L^1)_2(\mu\text{-}OH)_2](ClO_4)_2$ (1). The complex **1** (Figure 2) crystallizes in the monoclinic system with space group $C2/c$. The solved structure contains one dinuclear Zn^{II} complex with hydroxyl group and two halves of perchlorate anions in special position (2-fold axis). The asymmetric unit is linked to its 2-fold rotation equivalent through the O−H group to form a dimer.

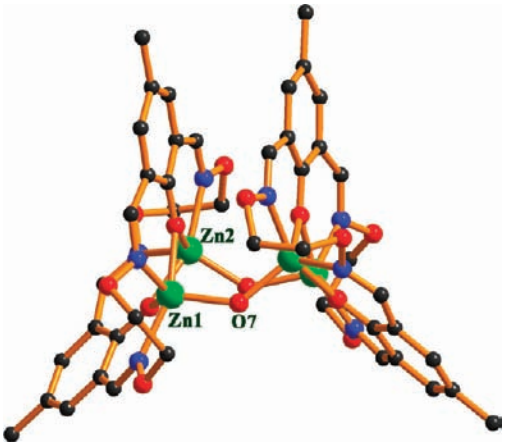

Figure 2. Dimeric structure of symmetrical macrocyclic dizinc(II) complex **1**. Hydrogen atoms and perchlorate anions are omitted for the sake of clarity.

The macrocyclic ligand is partially folded about the Zn···Zn axis. The approximate angle between the main planes of two halves (excluding the oxyimine planes) is 54.4 (2)°. The moiety (C1···C8, N1, N4) is less planar when compared to the other half (C12···C20, N2, N3). The atoms (C7 (0.113 Å), C8 (0.142 Å), N1 (0.125 Å), N4 (0.09 Å)) deviate much from the mean plane. Selected bond lengths and bond angles are summarized in Table S1, Supporting Information. The observed τ-parameters[23] of Zn1 (0.424) and Zn2 (0.344) centers indicated that each Zn^{II} ion adopts a distorted square pyramidal geometry. One of the outstanding features of this complex is the short intermetallic distance of 3.0469(11) Å, which is, in fact, a value much smaller than that the range typically encountered intermetallic distances in dinuclear zinc

dx.doi.org/10.1021/ic202451e | Inorg. Chem. 2012, 51, 5580−5592

sites of natural hydrolases (e.g., alkaline phosphatase, d(Zn···Zn) = 4.0 Å. The hydrogen atom of the hydroxyl group could not be located. However, the distance (2.886 Å) between hydroxyl group oxygen (O7) and O8_$1 ($1 = 1 − x, y, 1/2 − z) shows hydrogen bond interaction between the perchlorate anion and cation. Further, the packing (Figure S10 in the Supporting Information) is stabilized through intermolecular $\pi-\pi$ interaction between symmetry related (1.5 − x, 0.5y, −z) 4-methyl phenolate groups.

Description of Crystal Structure of $[Zn_2L^3(H_2O)_2](ClO_4)_2\cdot(H_2O)_3$ (3). The unsymmetrical macrocyclic dinuclear zinc(II) complex **3** (Figure 3) crystallizes in the orthorhombic

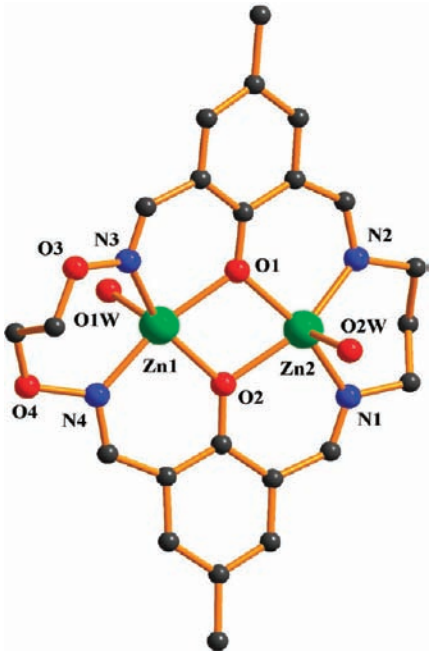

Figure 3. Crystal structure of unsymmetrical macrocyclic dizinc(II) complex **3**.

system with the space group *Pca*21. The unsymmetrical macrocyclic ligand containing each Zn^{II} ion is pentacoordinated, in which the equatorial plane of the oxyimine compartment is formed by two bridging phenoxide O atoms (O1 and O2) and two oxyimine N atoms (N3 and N4), while the basal plane of imine compartment is formed by the same two bridging phenoxide O atoms and two azomethine N atoms (N3 and N4).

Hydrogen atoms, crystal lattice containing water molecules, and perchlorate anions are omitted for the sake of clarity.

The list of selected bond lengths and angles are given in Table S2, Supporting Information. In both, the compartments containing Zn^{II} ions are axially coordinated with water molecules and completed their square pyramid geometry. The τ-parameters for geometry around Zn1 and Zn2 are 0.21 and 0.13, respectively. The distance between Zn···Zn centers is found to be 3.172 Å, which is longer than the Zn···Zn distance in symmetrical analogue **1** (3.047 Å). The packing (Figure S11 in the Supporting Information) of the molecule is stabilized through three-dimensional OH···O hydrogen bonds, mediated through solvent water and perchlorate anions. The trans angles at the Zn^{II} centers are deviated from 180°, ranging from 154.1(3) to 166.9(4). The Zn−O and Zn−N bond lengths lie in the range 2.023(9)−2.116(10) Å and 2.009(11) −2.110(10) Å respectively and the bond lengths are comparable to those observed in our early reported dicopper(II) complex of the same ligand.[15a] The two benzene rings in the molecule are parallel to each other, within the limits of standard deviations.

Phosphate Ester Hydrolysis. Many hydrolytic processes in enzyme−catalysis involve metal ions that are assumed to activate a water molecule which more easily forms a hydroxyl group as a nucleophile in the reaction system.[24] Presently, all the complexes **1**−**6** possess a potential nucleophile constituted by the metal coordinated water molecule in their structures and their catalytic activity on hydrolysis of 4-NPP ester was investigated. The dependence of the reaction rate of 4-NPP cleavage on pH in the presence of **1** and **4** is illustrated in Figure S12, Supporting Information. The value of k_{obs} increased as the pH increased from 6.0 to 8.0 and then decreased slightly at higher pH values, which gave a sigmoidal curve for the cleavage reaction. The data were fitted by the nonlinear least-squares method and gave the pH values above 6.8 at the inflection points corresponding to the pK_a values (Table 2)

Table 2. Kinetic Data for 4-NPP Hydrolysis and DNA Binding Parameters of the Dinuclear Zn^{II} Complexes

complex	pK_a	4-NPP hydrolysis 10^{-2} k_{cat} (s^{-1})	10^5 K_b [s][a]	10^5 K_{app}[b]	CD $\Delta\lambda_{max+}$ $\Delta\varepsilon$[c]
1	6.26	4.76 ± 0.09	3.3 [0.45]	2.94	−3(9)
2	6.59	2.16 ± 0.06	2.7 [0.32]	2.88	−3(6)
3	6.47	2.82 ± 0.10	2.1 [0.22]		−2(4)
4	6.41	3.46 ± 0.08	1.8 [0.19]		−2(3)
5	6.54	2.03 ± 0.11	5.2 [0.63]		−3(8)
6	6.49	2.54 ± 0.07	9.5 [0.82]	8.75	−4(12)

[a]Binding constants (M^{-1}) were determined by absorption spectrophotometric titration and [s] is the binding site size. [b]Apparent binding constants (M^{-1}) were determined by fluorescence spectrophotometric method. [c]$\Delta\lambda_{max}$ is the shift in nm of the positive DNA CD band at 274 nm. $\Delta\varepsilon$ (the value in parentheses) is the difference between the maximum ellipticity (in °) observed for the positive CD band in the spectrum of a 2:1 reaction mixture, and the ellipticity observed at the same wavelength in the spectrum of free CT DNA.

around 6.5 for one of the coordinated water molecules of **1**−**6**. It is noted that the complex **1** showed a maximum hydrolysis rate at pH 6.8 (pK_a = 6.26 ± 0.2) due to the presence of hydroxyl bridge between the two zinc(II) ions of two macrocyclic units. At pH 6.8, the hydroxyl bridges between the two macrocyclic units of symmetrical macrocyclic complex **1** are hydrolyzed[25] into water and hydroxyl ion coordinated two dinuclear intermediate species and form $[Zn_2L^1(H_2O)(OH^-)]$ species as the active catalyst for phosphate ester cleavage reaction. Similarly, the other unsymmetrical dizinc(II) complexes **2**−**6** containing each zinc(II) ion possess an axially coordinated water molecule. At higher pH conditions (>7), one of the coordinated water molecules gets deprotonated and forms the $[Zn_2L^{2\text{-}6}((H_2O)(OH^-)]$ species, which act as the active catalyst in the phosphate ester hydrolysis in a similar fashion to the active catalytic species $[Zn_2L^1(H_2O)(OH^-)]$ observed in complex **1**. Since the substrate concentration was essentially constant during the measurement, the initial first order rate constant (k_{obs}) was measured at different

dx.doi.org/10.1021/ic202451e | Inorg. Chem. 2012, 51, 5580−5592

concentrations of **1** and complexes **2**–**6** at pH 6.8 and 7.5, respectively. Plots of rate constant (k_{obs}) vs complex concentration are presented in Figure S13, Supporting Information. As can be seen, for all complexes, the rate of 4-NPP cleavage initially increases linearly with the increase of complex concentration, but gradually the reaction order in the complex concentration deviates from unity. In other words, the reaction exhibits a first order dependence only at low Zn^{II} complex concentrations. The first order rate constants k were obtained for the Zn^{II} complexes by analyzing Lineweaver–Burk plot, that is, $1/V_0$ vs $1/[4\text{-NPP}]$ by changing concentration of substrate (Figure 4) and the results of calculation are

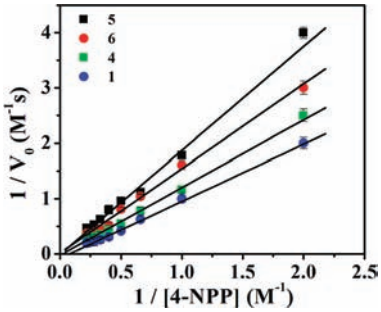

Figure 4. Lineweaver–Burk plot for the 4-NPP hydrolysis by Zn^{II} complexes **1**, **4**, **5**, and **6**.

summarized in Table 2. The study of the hydrolysis rate as a function of 4-NPP concentration shows a saturation behavior (Figure S14 in the Supporting Information). As can be observed for each complex, initially, the cleavage rate increases linearly with the increase of 4-NPP concentration but deviates gradually from linearity and finally tends toward a saturation curve. The data were treated using the Michaelis–Menten model, and the parameters V_{max}, k_M, and k_{cat} were obtained by nonlinear least-squares fits. The kinetic parameters for the hydrolysis of 4-NPP promoted by complexes **1**–**6** are described in Table S3, where it can be observed that complex **1** is most effective in the conversion of substrate to products. This may be due to the more electronegative oxygen atom attached to the imine nitrogens of both the compartments, which reduces the electron density around the metal ion and favors easy deprotonation of the metal coordinated water molecule. It has been assumed that the geometry around the zinc ions and the intermetallic distance are the two key factors that determine the catalytic activity of the complexes. Interestingly, the distance between Zn···Zn centers for **1** is found to be 3.047 Å, which is smaller than the unsymmetrical Zn^{II} analogue **3** (3.172 Å). The Zn···Zn distance also influenced the rate of phosphate ester hydrolysis reaction. From Table 2, it can be seen that the catalytic activity of the complexes (**2**, **3**, and **4**) are found to increase as the macrocyclic ring size increases, because of the intrinsic flexibility of the ligand makes the geometry around metal ion more distorted. It is evident from the literature[26] that the first order rate values for the more distorted complexes are higher than those of the less-distorted complexes. It is interesting that the catalytic activity of the aromatic diimine containing complexes (**5** and **6**) increases with increasing the chelation around zinc(II) ions. The first order rate values of the current dizinc(II) complexes are higher than the once previously reported[27] complexes given in Table 3.

Table 3. Calculated First Order Rate Constants for the Hydrolysis of Phosphate Esters by Previously Reported Zinc(II) Complexes

complex	substrate	k (s^{-1})	ref
$[Zn_2(LH_{-2})]^{2+}$	BNPP[a]	2.26×10^{-6}	27b
$[Zn(bpy)Cl_2]$	BNPP	5.74×10^{-7}	13c
[MPGN-Zn^{II}]	BNPP	3.60×10^{-5}	14a
$[Zn_2PBTPA]^{+}$	BNPP	2.30×10^{-8}	27c
$[Zn_2complex]$	HPNP[b]	4.00×10^{-7}	27d
$[Zn_2L_2O]^{3+}$	HPNP	4.10×10^{-3}	27e

[a]Bis(4-nitrophenyl)phosphate. [b]2-Hydroxypropyl(4-nitrophenyl)-phosphate.

DNA Binding. Absorption titration technique has been used to monitor the mode of interaction of **1**–**6** with CT DNA (Figure 5, Figure S15 in the Supporting Information).

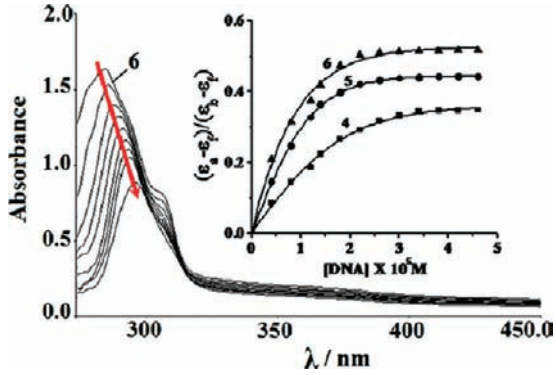

Figure 5. Absorption spectra of complex **6** (1×10^{-5} M) in the absence and presence of increasing amounts of CT–DNA (0–2.5×10^{-3} M) at 25 °C in 50 mM Tris–HCl/NaCl buffer (pH = 7.5). Arrow shows the absorbance changing upon increasing DNA concentrations. Insets shows the least–squares fit of $\Delta\varepsilon_{af}/\Delta\varepsilon_{bf}$ vs [DNA] for the complexes **4**–**6**.

The DNA binding constant (K_b) values of the complexes along with the binding site size (s) are given in Table 2. The K_b values of $\sim 10^5$ M^{-1} follow the order: **6** > **5** > **1** > **2** > **3** > **4**. The naphthalene diimine containing complex **6** show higher K_b values in comparison to their other analogues possibly due to the coplanarity of the naphthalene system in the macrocyclic ring.[13a,27a] Interestingly, the complex **1** also showed better DNA binding propensity than the other aliphatic diimine containing complexes **2**–**4**. This is due to the rigid nature[28] of the oxime group in both the compartments which favors stronger interaction with DNA than the other aliphatic diimines. The s value gives a measure of the number of DNA bases associated with the complex and an s value of <1 typically arises because of aggregation of hydrophobic molecules on the DNA surface.[29] We have used the fluorescence spectral (Figure S16–S17, Supporting Information) titration method to obtain the apparent binding constant values (K_{app}) of **1**, **2**, and **6**. EB has been used as a spectral probe as it exhibits enhanced emission intensity when it binds to the DNA. The competitive binding of the complexes to DNA could result in the displacement of the bound EB and could cause decrease in the emission intensity because of solvent quenching. The K_{app} values (Table 2) of the complexes are $\sim 10^5$ M^{-1}. The CD spectral method was used to access the conformational changes induced by **1**–**6** in DNA.[30] CT DNA exhibits positive band at

dx.doi.org/10.1021/ic202451e | Inorg. Chem. 2012, 51, 5580–5592

272 nm (UV: λ_{max} = 260 nm) due to base stacking and negative band at 239 nm due to helicity of B−DNA.[31] It was reported[32] that the change in elipticity and shifting to higher energy of the positive CD signals are due to intercalative mode of binding. Incubation of the DNA with **1**−**6** induced considerable changes in CD spectrum (Figure S18 in the Supporting Information). Examination of Table 2 shows that the magnitude of the increase in elipticity at 272 nm increases in the following order **4** < **3** < **2** < **1** < **5** < **6**. The result reveals that the changes induced by **5** and **6** are more significant than those by **1**−**4**, which suggests that **6** has higher affinity for CT DNA than **1**−**4** does. Viscosity measurements have been carried out to examine the effect of the complexes on the specific relative viscosity of DNA. Since the relative specific viscosity (η/η_0) of DNA gives a measure of the increase in contour length associated with the separation of DNA base pairs caused by intercalation, a classical DNA intercalator like EB shows a significant increase in the viscosity of the DNA solutions (η and η_0 are the specific viscosities of DNA in the presence and absence of the complexes, respectively). In contrast, a partial and/or non-intercalation of the complex could result in a less pronounced effect on the viscosity.[33] The effects of **1**, **4**, **6**, and EB on the viscosity of rod-like DNA are shown in Figure 6.

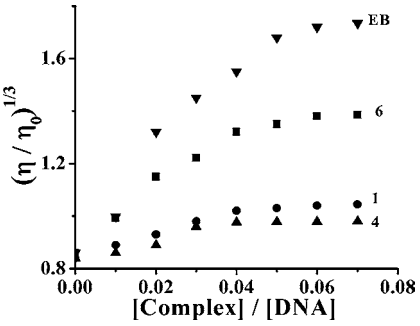

Figure 6. Effect of increasing amounts of EB (a), Zn^{II} complexes **1**, **4**, and **6** on the relative viscosity of calf thymus DNA at 25 (±0.1) °C. The total concentration of DNA is 0.5 mM.

Complexes **1** and **4** bind by electrostatic interactions only and exerted essentially no such effect. After the amounts of **6** were increased, the relative viscosity of DNA increases steadily, similar to EB. The increase in relative viscosity, expected to correlate with the compound's DNA−intercalating potential, followed the order EB > **6** > **1** > **4**. These results suggest that complex **6** can bind to DNA through intercalation, due to the presence of the naphthalene ring system in one compartment of the ligand $\mathbf{L}^6$.

DNA Cleavage Activity. The hydrolytic DNA cleavage activity of $\mathbf{L}^1$, [**ZnL**], and **1**−**6** have been studied using SC pBR322 DNA in a medium of Tris−HCl/NaCl buffer (pH 7.0) in dark conditions (Figure 7). A 20 μM solution of the complexes shows essentially complete cleavage of SC DNA (0.33 μg) on 45 min incubation at 37 °C. $\mathbf{L}^1$ and Zn^{II} ions do not show any considerable DNA cleavage. As expected, naphthalene diimine containing complex **6** showed significantly enhanced DNA cleavage activity than all other mono- and dinuclear analogues. Figure S19 in the Supporting Information shows that there is no evident inhibition effect on the DNA cleavage in the presence of all scavengers, which rules out the involvement of these reactive oxygen species, at least in a free and diffusible form. The oxygen-independent pathway is also

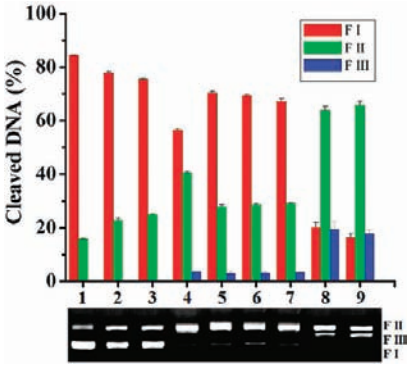

Figure 7. Cleavage of SC pBR322 DNA (0.2 μg, 33.3 μM) by complexes **1**−**6** (20 μM) in 50 mM Tris−HCl/NaCl buffer (pH 7.0). Lane 1, DNA control; lane 2, DNA + $Zn(ClO_4)_2{\cdot}6H_2O$ (20 μM); lane 3, DNA + L^1 (20 μM); lanes 4−9, DNA + dizinc(II) complexes **1**−**6**, respectively.

evidenced from the observation of significant DNA cleavage under an argon atmosphere. On the other hand, zinc(II) complexes generally cleave DNA by the hydrolytic pathway.[34] To ascertain the hydrolytic nature of the cleavage reaction enhanced by **5** and **6**, the linear form (F−III) obtained from the cleavage of SC DNA (F−I) was reacted with T4 ligase enzyme, and we have observed complete conversion of the linear DNA to its circular relaxed form (F−II) (Figure S20 in the Supporting Information). To further prove the hydrolysis pathway, a small dinucleotide model system adenylyl(3′−5′)phosphoadenine (ApA) was used as the nucleic acid mimic. ApA (0.10 mM) and 2.5% DMF solution of **1** (0.01 mM) were dissolved in deionized water, and after equilibration for 8 h at r.t. ESI−MS analysis was carried out. In the ESI−MS spectrum (Figure 8), the signals at m/z 268.07 and 347.40 show the

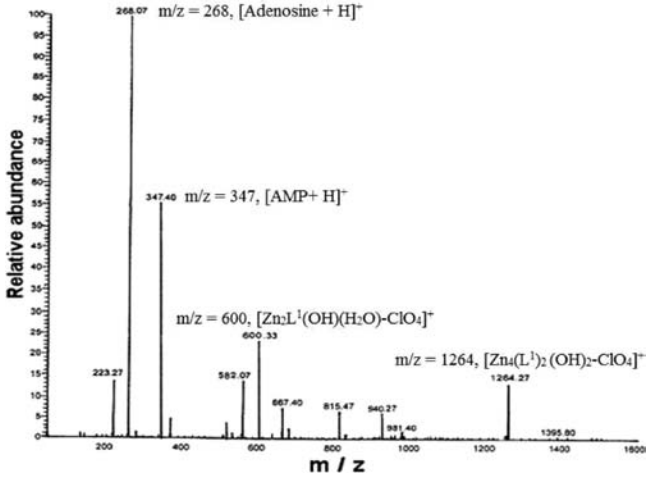

Figure 8. ESI−MS analysis of ApA hydrolysis promoted by complex **1**.

presence of ApA cleavage products adenosine (calcd m/z 268.10) and adenine monophosphate (AMP, calcd m/z 348.06). The generation of the adenosine and AMP indicates that the phosphodiester bonds of ApA were cleaved by **1** via the hydrolytic pathway.[35] Therefore, as in ApA, the hydrolysis pathway should be the possible mechanism for DNA cleavage promoted by **1**. As a comparison, ESI−MS analysis of ApA treated with $\mathbf{L}^1$ was also carried out under the same conditions (Figure S21 in the Supporting Information), and there were no

dx.doi.org/10.1021/ic202451e | Inorg. Chem. 2012, 51, 5580−5592

signs of cleavage products (adenosine and AMP). Because of its neutral nature, we have not performed ESI−MS analysis of ApA hydrolysis promoted by [ZnL]. However, the observed rate constants of dizinc(II) complexes **1** and **6** for DNA hydrolysis are around 10 times faster than the mononuclear Zn^{II} complex [ZnL]. Therefore, investigation of the ApA hydrolysis clearly indicates that the acceleration by dizinc(II) complex **1** is due to the cooperative catalysis of the two proximate Zn^{II} centers.[14c−e] The ESI−MS spectrum of **1** supports the existence of the zinc(II)-bound OH^- in the solution (Scheme 2). This fact is also consistent with the result

Scheme 2. Equilibration between A and B

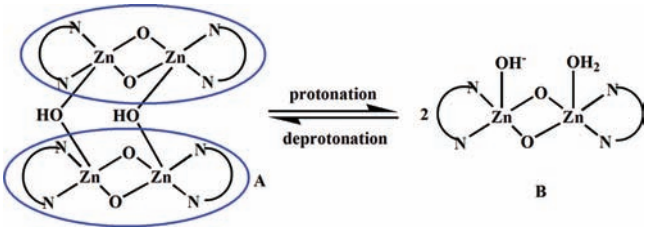

reported by Sheng and co-workers.[14c] Therefore, a similar status is achieved in the dinuclear zinc(II) complex presented here. According to some reports from the literature,[36] a plausible mechanism for DNA cleavage promoted by macrocyclic dizinc(II) complex is schematically depicted in Scheme 3. It is well-known that bimetallic complexes bind the phosphodiester backbone of DNA tightly due to the two-point DNA binding mechanism.[37]

Therefore, the first step of DNA cleavage promoted by dizinc(II) complex is that in which two zinc(II) cations recognize and bind the phosphodiester bond of DNA through the coordinate linkage and electrostatic interaction, and the synergistic effect between the two zinc(II) ions activate the central phosphorus atom. Then, the activated phosphorus atom is nucleophilically attacked by the proximate zinc(II)-bound OH, resulting in the formation of the trigonal bipyramidal phosphorus intermediate. Finally, one of the P−O ester bonds of the DNA is cleaved and catalyst is regenerated. In order to assess whether the DNA cleavage enhancement is due to ligand or number of metal centers dependent, we have performed time course measurements for mono, aliphatic, and aromatic diimine containing macrocyclic dinuclear complexes [**ZnL**], **1** and **6**, respectively. In order to determine the hydrolytic cleavage rate, the kinetic aspects of the hydrolytic DNA cleavage have been investigated. Reactions were carried out under pseudo-Michaelis−Menten conditions by using various concentrations of [**ZnL**], **1**, and **6** (Figure S22 in the Supporting Information).

On the basis of the plots of k_{obs} vs concentration of complexes, the pseudo-Michaelis−Menten kinetic parameters were calculated to be $k_{cat} = 0.36 \pm 0.1\ h^{-1}$, $K_M = 0.52 \pm 10^{-3}$ M for [ZnL], $k_{cat} = 2.67 \pm 0.1\ h^{-1}$, $K_M = 3.73 \pm 10^{-2}$ M for **1** and $k_{cat} = 4.42 \pm 0.2\ h^{-1}$, $K_M = 5.5 \pm 10^{-2}$ M for **6**. It is noted that the complex **6** displayed a 12-fold higher DNA hydrolysis rate compared to the mononuclear complex [**ZnL**]. The complex **6** also shows an enormous enhancement of the cleavage rate of 1.23×10^8 in comparison to the uncatalyzed hydrolysis rate ($k = 3.6 \times 10^{-8}\ h^{-1}$) of ds-DNA. This rate enhancement is significantly higher than those reported for transition metal-based synthetic hydrolases[14] but less when compared to Mg-EcoRV or Mn-EcoRV ($\sim 1.3 \times 10^9$).[38] By comparing the results of hydrolysis reactions catalyzed by [**ZnL**], **1**, and **6**, we can conclude that the macrocyclic ligand with more aromatic moiety and hard Lewis acid properties of Zn^{II} ions could play an important role in the DNA cleavage process.

Scheme 3. A Plausible Mechanism for DNA Cleavage Promoted by Zn^{II} Complexes

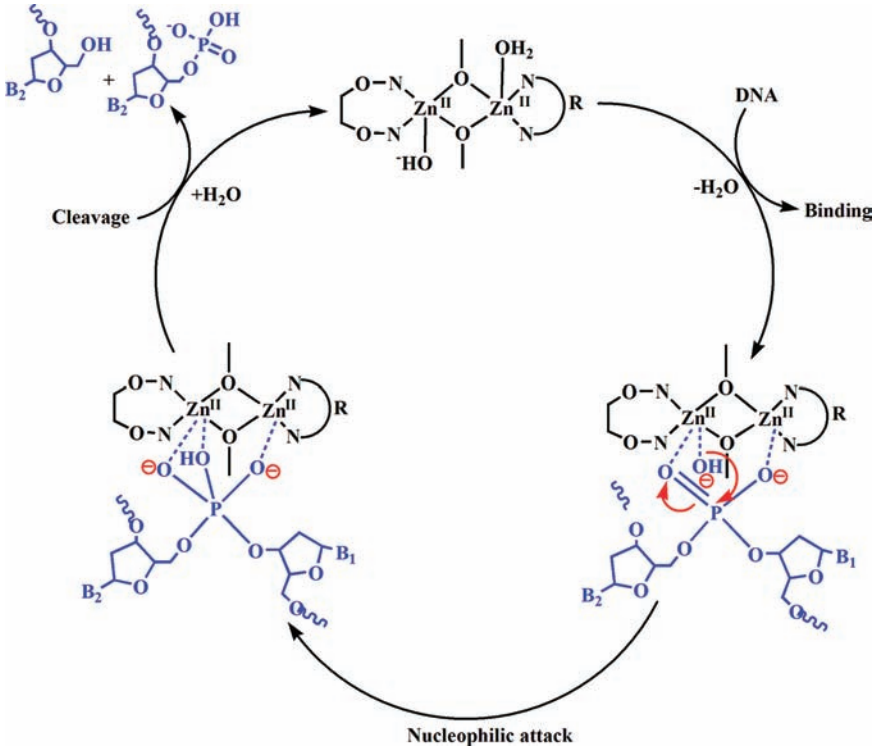

dx.doi.org/10.1021/ic202451e | Inorg. Chem. 2012, 51, 5580−5592

The observed kinetic parameters for DNA hydrolysis by current macrocyclic dizinc(II) complexes are higher than our previously reported dinickel(II) analogues.[15b] It is well-known in the literature[39] that zinc(II) ion is a more efficient Lewis acid than nickel(II) ion. Thus the hard Lewis acid properties allow Zn^{II} ions to vastly accelerate the rate of phosphate ester hydrolysis[40] by coordinating a phosphoryl oxygen of DNA compared to Ni(II) ions.

Cytotoxic Activity. Hydrolysis of the phosphodiester bond of DNA is crucial at several stages in the cell cycle, including DNA repair and excision, integration, and signal transduction.[41] Meanwhile, the hydrolytic damage of the DNA backbone has been reported to be related to antitumor potential,[42] which prompts us to evaluate the cytotoxicity of $\mathbf{L^1}$, **1**, **3**, and **6** toward HepG2 cell lines by the MTT assay. HepG2 cells were exposed to different concentrations of Zn^{II} ion, $\mathbf{L^1}$, **1**, **3**, and **6** for 48 h. As shown in Figure 9, the complexes cause dose-dependent cytotoxicity in the range of 10−100 μM with approximately 50% of the cells (IC_{50}) having lost viability after being treated with $\mathbf{L^1}$, **1**, **3**, and **6** at the concentration of 117, 16.5, 37.1, and 8.32 μM, respectively. Besides, the antitumor performance of Zn^{2+} ions in 48 h was also investigated, and it did not induce apparent changes compared to that of **1**, **3**, and **6**. The antitumor activities are shown to follow the order $\mathbf{Zn^{II}} < \mathbf{L^1} < \mathbf{3} < \mathbf{1} < \mathbf{6}$. Heavy metal ions are cytotoxic to cells at 10^{-3} M.[43] Figure 10 shows that zinc(II) ions also exhibit antitumor activity at this level, but when zinc(II) ions are diluted to 3×10^{-4} M, the percentage inhibition decreases sharply (IC_{50}) 3.34×10^{-4} M. We noticed that the IC_{50} value against HepG2 cells of complex **6** is 45-fold larger than that of $\mathbf{L^1}$. Remarkably, it exhibits the highest activity against HepG2 cells with an IC_{50} value of 8.32 μM, and also exhibits potency higher than the cisplatin (IC_{50}, 21.5 μM)[44] against the same cell lines and under identical experimental conditions.

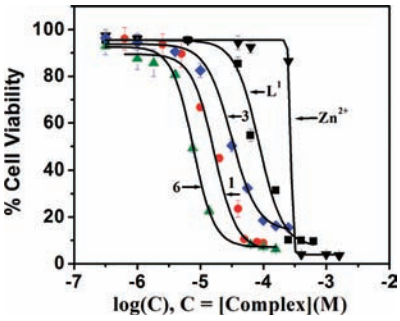

Figure 9. Inhibitory effect of zinc(II) ion, ligand $\mathbf{L^1}$, and dizinc complexes **1**, **3**, and **6** on the proliferation of HepG2 cells. Cells were exposed to the compounds for 48 h. The relative survival rate was determined in relation to that of untreated control cells, which was set to 100%. Data are means of the standard deviation of three experiments, and each experiment included triplicate wells.

Fluorescent Staining Method. The characteristic morphological changes brought about in the cells by treatment with Zn^{II} ion, $\mathbf{L^1}$, **1**, **3**, and **6** have been evaluated by adopting fluorescent microscopic analysis Annexin V-FITC stained cells. The control viable cells have uniformly green fluorescing nuclei and a highly organized structure. After cells were treated with IC_{50} concentration of the complexes **1**, **3**, and **6** for 48 h, we have observed cytological changes like late apoptotic cells that have orange to red fluorescing nuclei (Figure 10) with condensed or fragmented chromatin and necrotic cells, swollen to large sizes that have uniformly orange to red fluorescing nuclei with no indication of chromatin fragmentation by staining. The results indicate that the complexes **1**, **3**, and **6** induce cell death through necrosis or apoptosis compared with Zn^{II} ion and ligand $\mathbf{L^1}$. According to these results of the cytotoxic assays, we conclude that the complex **6** exhibits much stronger cytotoxic effects than complexes **1** and **3**.

Flow Cytometric Analysis of HepG2 Cell Cycle Distribution and Apoptosis. To investigate the mechanism of cell division and cell death induced by ligand $\mathbf{L^1}$, **1**, **3**, and **6** on HepG2 cells, we employed the fluorescence-activated cell sorting (FACS) analysis of the DNA content. The cell cycle progression was analyzed at 48 h incubation time with IC_{50} concentrations of $\mathbf{L^1}$, **1**, **3**, and **6**, and the results are depicted (Figure S23 in the Supporting Information). In the control experiments, 2.4% of the cells were found to be populated at sub-G0/G1 (apoptotic) phase for the incubation period 48 h,

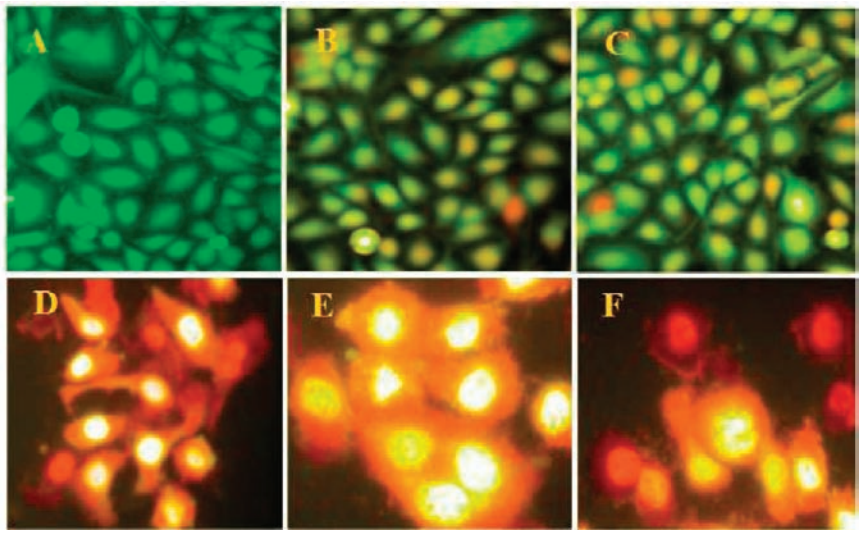

Figure 10. Annexin V-FITC stained HepG2 cancer cells. (A) Untreated cells (in 0.01% DMSO), (B) treatment of $Zn(ClO_4)_2 \cdot 6H_2O$, (C) ligand $\mathbf{L^1}$ and (D−F) treatment of complexes **1**, **3** and **6** − IC_{50}, respectively at 48 h of incubation.

dx.doi.org/10.1021/ic202451e | Inorg. Chem. 2012, 51, 5580−5592

and also, higher percentage of cells were populated at the G0/G1 phase (78.2% at 48 h) and lower percentage of cells were populated at the S phase and G2/M phases. It is well-known that in this analysis, the cells in the G0/G1 phase have unreplicated diploid (2n) DNA content, whereas the G2/M phase has replicated ploid (4n) DNA. Also, hypodiploidy (<2n) DNA content at the sub-G0/G1 phase and replication in the S phase are observable.

Upon exposure of the cells to $\mathbf{L}^1$, **1**, **3**, and **6**, the accumulation of cells increased in the sub-G0/G1 phase from 2.4% (control) to 14.2, 42.5, 26.6 and 62.4% at 48 h, respectively, and thus the percentage of cells accumulated at this phase increased with increasing the aromatic moiety in macrocyclic ligand. Also, the percentage of cells decreased in the remaining phases of the cell cycle (G0/G1 phase from 78.2% (control) to 74.2, 36.4, 64.8, and 35.4%; S phase, from 8.2% (control) to 4.2, 2.8, 3.4 and 0.8%; G2/M from 11.2 to 7.4, 3.3, 5.2 and 1.4%) with incubation time, indicating blockage of cell progression into G0/G1, S, and G2/M phases and hence inhibition of DNA replication.[45] The cell cycle analysis of HepG2 after treatment of $\mathbf{L}^1$, **1**, **3**, and **6** revealed an increase in the subdiploidal population which represent cells with significant DNA damage, indicating a late apoptotic stage.[46]

Western Blot Analysis of Caspase-3/-9 Activation. The caspases are a family of cysteine proteases which participate in a cascade triggered by pro-apoptotic signals and culminates in the cleavage of a set of proteins, resulting in disassembly of the cells.[47] Caspase-3 is a well-known downstream adaptor caspase which can be proteolytically activated by caspase-9 via mitochondrial or cell death receptor signaling pathways.[48]After After 48 h exposure to $\mathbf{L}^1$, **1**, **3**, and **6** at IC_{50} concentrations, it was found that caspase-3 activity increased from 18% to 84% and caspase-9 activity from 22% to 94% were cleaved to their active forms in a ligand-dependent manner (Figure S24 in the Supporting Information). It is noted that the complex **6** displayed better activation of caspase-3 and caspase-9 than $\mathbf{L}^1$, **1**, and **3**. This result reveals that the complexes are activating caspase-3 and -9 through mitochondria-mediated intrinsic pathway, which led to internucleosomal DNA fragmentation in HepG2 cells.[49]

LDH Inhibition Activity. The cytoplasmic enzyme (LDH), which catalyzes the oxidation of lactate to pyruvate and vice versa, is also a known marker of membrane integrity and a regulator of vital biochemical reactions.[50] The quantity of LDH has been analyzed in HepG2 cell lysate as well as in conditioned media for 48 h treatment of $\mathbf{L}^1$, **1**, **3**, and **6**. The LDH was significantly decreased in cell lysate when compared to control cells with $\mathbf{L}^1$, **1**, **3**, and **6** treated cells (IC_{50} concentrations) (Figure S25 in the Supporting Information). The activity of LDH was significantly increased in conditioned media when compared with controlled cells. This confirms the cytotoxic ability of $\mathbf{L}^1$, **1**, **3**, and **6** against the HepG2 cells. Because of the apoptosis induced by $\mathbf{L}^1$, **1**, **3**, and **6**, the membrane permeability increases, and hence there is a leakage of LDH from the cells into the medium. The complex **6** caused significant LDH leakage ($p < 0.05$) as compared with $\mathbf{L}^1$, **1**, **3**, and control. This results in the content of LDH increasing in conditioned media and decreasing in the cell lysate.

CONCLUSIONS

A series of macrocyclic dizinc(II) complexes have been synthesized and their catalytic, DNA binding, DNA hydrolysis, cytotoxic properties were also evaluated. The rate of phosphate ester hydrolysis increased with increasing macrocyclic ring size of the complexes. Introducing and extending the aromatic moiety in the macrocyclic ring led to considerable changes in DNA binding mode and hydrolysis rate under physiological conditions. The complex **6** displayed higher DNA binding propensity (intercalative mode) and cleavage activity than the other dizinc(II) analogues. Remarkably, the complex **6** exhibited the highest activity against HepG2 cells with an IC_{50} value of 8.32 μM, and also exhibited potency higher than the widely used drug cisplatin (IC_{50}, 21.5 μM) against the same cell lines. This reveals that a synergic combination of the ligand and metal ion is important in the design of a potential anticancer drug, the activity of which correlates well with the ability of the complexes to strongly bind and cleave DNA. Thus, the stacking interaction exhibited by the naphthalene diimine containing macrocyclic ligand $\mathbf{L}^6$, which is responsible for the stronger DNA intercalative binding, more effective DNA cleavage of the complex in the absence of any additives, and more facile transport across the cell membrane of the complex **6**, accounts for the enhanced cytotoxicity of the complex. Also, biochemical studies related to cytotoxicity reveal that the complexes **1** and **6** acts as potent anticancer agent by inducing phenotypical changes, increasing membrane permeability, and activation of caspase-3 and -9, which is consistent with the induction of mainly apoptotic cell death. Further, mechanistic and cellular uptake studies are essential to probe the higher potency of the complex to kill cancer cells.

ASSOCIATED CONTENT

Supporting Information

X-ray crystallographic files in CIF format and additional structural, phosphate ester hydrolysis, DNA binding, cleavage and cytotoxicity data for the complexes are available.This material is available free of charge via the Internet at http://pubs.acs.org.

AUTHOR INFORMATION

Corresponding Author

*E-mail: mkands@yahoo.com.

Notes

The authors declare no competing financial interest.

ACKNOWLEDGMENTS

S.A. is grateful to CSIR, New Delhi, Government of India, for a fellowship (SRF). The authors thank the Department of Science and Technology (DST-FIST), New Delhi, Government of India, for financial support. S.A. is thankful to Arun Kumar Bar, IPC Department, IISc, Bangalore, for solving one of the crystal structures.

REFERENCES

(1) (a) Lippard, S. J. *Pure Appl. Chem.* **1987**, *59*, 731. (b) Fuertes, M. A.; Alonso, C.; Perez., J. M. *Chem. Rev.* **2003**, *103*, 645. (c) Lippert, B. *Cisplatin: Chemistry and Biochemistry of a Leading Anticancer Drug*; Lippert, B., Ed.; Wiley−VCH Verlag GmbH: Weinheim, Germany, 1999.

(2) (a) Bales, B. C.; Kodama, T.; Weledji, Y. N.; Pitie, M.; Meunier, B.; Greenberg, M. M. *Nucleic Acid Res.* **2005**, *33*, 5371. (b) Wang, D.; Lippard, S. J. *Nat. Rev. Drug Discovery* **2005**, *4*, 307. (c) Frezza, M.; Hindo, S. S.; Tomco, D.; Allard, M. M.; Cui, Q. C.; Heeg, M. J.; Chen, D.; Dou, Q. P.; Verani, C. N. *Inorg. Chem.* **2009**, *48*, 5928. (d) Clarke,

M. J.; Zhu, F.; Frasca, D. R. *Chem. Rev.* **1999**, *99*, 2511. (e) Jamieson, E. R.; Lippard, S. *J. Chem. Rev.* **1999**, *99*, 2467.
(3) (a) Djeković, A.; Petrović, B.; Bugarčić, Ž. D.; Puchta, R.; van Eldik, R. *Dalton Trans.* **2012**, *40*, 3633. (b) Clarke, M. J.; Zhu, F.; Frasca, D. R. *Chem. Rev.* **1999**, *99*, 2511. (c) Ott, I.; Gust, R. *Arch. Pharm.* **2007**, *340*, 117. (d) Bruijnincx, P. C.; Sadler, P. J. *Curr. Opin. Chem. Biol.* **2008**, *12*, 197.
(4) (a) Ramakrishnan, S.; Rajendiran, V.; Palaniandavar, M.; Periasamy, V. S.; Srinag, B. S.; Krishnamurthy, H.; Akbarsha, M. A. *Inorg. Chem.* **2009**, *48*, 1309. (b) Ramakrishnan, S.; Shakthipriya, D.; Suresh, E.; Periasamy, V. S.; Akbarsha, M. A.; Palaniandavar, M. *Inorg. Chem.* **2011**, *50*, 6458. (c) Splith, K.; Hu, W.; Schatzschneider, U.; Onambele, L. A.; Prokop, A.; Gust, R.; Ott, I.; Neundorf, I. *Bioconjugate Chem.* **2010**, *21*, 1288. (d) Hille, A.; Ott, I.; Kitanovic, A.; Kitanovic, I.; Alborzina, H.; Lederer, E.; Wölfl, S.; Metzler-Nolte, N.; Schäfer, S.; Sheldrick, W. S.; Bischof, C.; Schatzschneider, U.; Gust, R. *J. Biol. Inorg. Chem.* **2009**, *14*, 711. (e) Reisner, E.; Arion, V. B.; Guedes da Silva, M. F. C.; Lichtenecker, R.; Eichinger, A.; Keppler, B. K.; Kukushkin, V. Yu.; Pombeiro, A. J. L. *Inorg. Chem.* **2004**, *43*, 7083.
(5) (a) Thorp, H. H. *Chem. Biol.* **1998**, *5*, R125. (b) Vahrenkamp, H. *Dalton Trans.* **2007**, 4751. (c) Anzellotti, A. I.; Farrell, N. P. *Chem. Soc. Rev.* **2008**, *37*, 1629.
(6) Emami, S.; Hosseinimehr, S. J.; Taghdisi, S. M.; Akhlaghpoor, S. *Bioorg. Med. Chem. Lett.* **2007**, *17*, 45.
(7) Huang, Q.; Pan, Z.; Wang, P.; Chen, Z.; Zhang, X.; Xu, H. *Bioorg. Med. Chem. Lett.* **2006**, *16*, 3030.
(8) (a) Nakayama, A.; Hiromura, M.; Adachi, Y.; Sakurai, H. *J. Biol. Inorg. Chem.* **2008**, *13*, 675. (b) Sakurai, H.; Yoshikawa, Y.; Yasui, H. *Chem. Soc. Rev.* **2008**, *7*, 2383.
(9) (a) Chohan, Z. H.; Arif, M.; Sarfraz, M. *Appl. Organomet. Chem.* **2007**, *21*, 294. (b) Singh, V. P.; Katiyar, A. *J. Coord. Chem.* **2008**, *61*, 3200. (c) Kaczmarek, M. T.; Jastrza, R.; Hołderna-Kedzia, E.; Radecka-Paryzek, W. *Inorg. Chim. Acta* **2009**, *362*, 3127.
(10) Ali, M. M.; Frei, E.; Straubb, J.; Breuerb, A.; Wiesslerb, M. *Toxicology* **2002**, *85*, 179.
(11) (a) Miyamoto, D.; Endo, N.; Oku, N.; Arima, Y.; Suzuki, T.; Suzuki, Y. *Biol. Pharm. Bull.* **1998**, *21*, 1258. (b) Ferrari, M. B.; Bisceglie, F.; Pelosia, G.; Tarasconia, P.; Albertini, R.; Pinelli, S. *J. Inorg. Biochem.* **2001**, *87*, 137. (c) Beraldo, H.; Gambinob, D. *Mini-Rev. Med. Chem.* **2004**, *4*, 31. (d) Zhang, H.; Liu, C. S.; Bu, X. H.; Yang, M. *J. Inorg. Biochem.* **2005**, *99*, 1119. (e) Tan, J.; Wang, B.; Zhu, L. *Bioorg. Med. Chem.* **2009**, *17*, 614. (f) Jiang, Q.; Zhu, J.; Zhang, Y.; Xiao, N.; Guo, Z. *BioMetals* **2009**, *22*, 297. (g) Wen, J.-H.; Li, C.-Y.; Geng, Z.-R.; Ma, X.-Y.; Wang, Z.-L. *Chem. Commun.* **2011**, *47*, 11330.
(12) (a) Maheswari, P. U.; Barends, S.; Yaman, S. O.; Hoog, P.; Casellas, H.; Teat, S. J.; Massera, C.; Lutz, M.; Spek, A. L.; vanWezel, G. P.; Gamez, P.; Reedijk, J. *Chem.—Eur. J.* **2007**, *13*, 5213. (b) Li, J. H.; Wang, J. T.; Mao, Z. W.; Ji, L. N. *Inorg. Chem. Commun.* **2008**, *11*, 865. (c) Bazzicalupi, C.; Bencini, A.; Bianchi, A.; Biver, T.; Boggioni, A.; Bonacchi, S.; Danesi, A.; Giorgi, C.; Gratteri, P.; Ingraín, A. M.; Secco, F.; Sissi, C.; Valtancoli, B.; Venturini, M. *Chem.—Eur. J.* **2008**, *14*, 184. (d) Wang, J.; Yang, Z.−Y.; Yi, X.−Y.; Wang, B.−D. *J. Photochem. Photobiol. A* **2009**, *201*, 183. (e) Shi, Y.; Toms, B. B.; Dixit, N.; Kumari, N.; Mishra, L.; Goodisman, J.; Dabrowiak, J. C. *Chem. Res. Toxicol.* **2010**, *23*, 1417.
(13) (a) Fitzsimons, M. P.; Barton, J. K. *J. Am. Chem. Soc.* **1997**, *119*, 3379. (b) Liguori, P. F.; Valentini, A.; Palma, M.; Bellusci, A.; Bernardini, S.; Ghedini, M.; Panno, M. L.; Pettinari, C.; Marchetti, F.; Crispini, A.; Pucci, D. *Dalton Trans.* **2010**, *39*, 4205. (c) He, J.; Sun, J.; Maoa, Z.−W.; Ji, L.−N.; Sun, H. *J. Inorg. Biochem.* **2009**, *103*, 851. (d) Kuang, G.−C.; Allen, J. R.; Baird, M. A.; Nguyen, B. T.; Zhang, L.; Morgan, T. J., Jr; Levenson, C. W.; Davidson, M. W.; Zhu, L. *Inorg. Chem.* **2011**, *50*, 10493. (e) Peralta, R. A.; Bortoluzzi, A. J.; de Souza, B.; Jovito, R.; Xavier, F. R.; Couto, R. A. A.; Casellato, A.; Nome, F.; Dick, A.; Gahan, L. R.; Schenk, G.; Hanson, G. R.; de Paula, F. C. S.; Maia, E. C. P.; Machado, S. P.; Severino, P. C.; Pich, C.; Bortolotto, T.; Terenzi, H.; Castellano, E. E.; Neves, A.; Riley, M. J. *Inorg. Chem.* **2010**, *49*, 11421. (f) Liu, C. T.; Neverov, A. A.; Brown, R. S. *J. Am. Chem. Soc.* **2008**, *130*, 13870. (g) Asayama, S.; Nishinohara, S.; Kawakami, H. *Bioconjugate Chem.* **2011**, *22*, 1864.
(14) (a) Bonomi, R.; Selvestrel, F.; Lombardo, V.; Sissi, C.; Polizzi, S.; Mancin, F.; Tonellato, U.; Scrimin, P. *J. Am. Chem. Soc.* **2008**, *130*, 15744. (b) Lombardo, V.; Bonomi, R.; Sissi, C.; Mancin, F. *Tetrahedron* **2010**, *66*, 2189. (c) Sheng, X.; Guo, X.; Lu, X. M.; Lu, G. Y.; Shao, Y.; Liu, F.; Xu, Q. *Bioconjugate Chem* **2008**, *19*, 490. (d) Iranzo, O.; Elmer, T.; Richard, J. P.; Morrow, J. R. *Inorg. Chem.* **2003**, *42*, 7737. (e) Peng, W.; Liu, P.-Y.; Jiang, N.; Lin, H.-H.; Zhang, G.-L.; Liu, Y.; Yu, X.-Q. *Bioorg. Chem.* **2005**, *33*, 374.
(15) (a) Anbu, S.; Kandaswamy, M.; Suthakaran, P.; Murugan, V.; Varghese, B. *J. Inorg. Biochem.* **2009**, *103*, 401. (b) Anbu, S.; Kandaswamy, M.; Varghese, B. *Dalton Trans.* **2010**, *39*, 3823. (c) Leelavathy, L.; Anbu, S.; Kandaswamy, M.; Karthikeyan, N.; Mohan, N. *Polyhedron* **2009**, *28*, 903. (d) Anbu, S.; Kandaswamy, M.; Moorthy, P. S.; Balasubramanian, M.; Ponnuswamy, M. N. *Polyhedron* **2009**, *28*, 49. (e) Anbu, S.; Kandaswamy, M. *Polyhedron* **2011**, *30*, 123. (f) Anbu, S.; Kandaswamy, M.; Selvaraj, M. *Polyhedron* **2012**, *33*, 1. (g) Anbu, S.; Kandaswamy, M. *Inorg. Chim. Acta* **2012**, *385*, 45. (h) Anbu, S.; Shanmugaraju, S.; Kandaswamy, M. *RSC Adv.* DOI: 10.1039/C2RA20228J.
(16) Anbu, S.; Kandaswamy, M.; Kamalraj, S.; Muthumarry, J.; Varghese, B. *Dalton Trans.* **2011**, *40*, 7310.
(17) Verani, N. V.; Rentschler, E.; Weyhermuller, T.; Bill, E.; Chaudhuri, P. *J. Chem. Soc., Dalton Trans.* **2000**, 251.
(18) Dixon, D. W.; Weiss, R. H. *J. Org. Chem.* **1984**, *49*, 4487.
(19) Merill, C.; Goldman, D.; Sedman, S. A.; Ebert, M. H. *Science* **1980**, *211*, 1437.
(20) Wolsey, W. C. *J. Chem. Educ.* **1973**, *50*, A335.
(21) Subat, M.; Woinaroschy, K.; Anthofer, S.; Malterer, B.; Konig, B. *Inorg. Chem.* **2007**, *46*, 4336.
(22) King, J. C. *Practical Clinical Enzymology*; D. von Nostrand Co.: London, 1965.
(23) Addison, A. W.; Rao, T. N.; Reedijk, J.; Van Rijn, J.; Verschoor, G. C. *J. Chem. Soc., Dalton Trans.* **1984**, 1349.
(24) (a) Rey, N. A.; Neves, A.; Bortoluzzi, A.; Pich, C. T.; Terenzi, H. *Inorg. Chem.* **2007**, *46*, 348. (b) Belle, C.; Beguin, C.; Luneau, I. G.; Hamman, S.; Philouze, C.; Pierre, J. L.; Thomas, F.; Torelli, S. *Inorg. Chem.* **2002**, *41*, 479. (c) Hongjun, W.; Min, H.; Chengtai, W. *Wuhan Univ. J. Nat. Sci.* **1997**, *2*, 321.
(25) Deal, K. A.; Burstyn, J. N. *Inorg. Chem.* **1996**, *35*, 2792.
(26) (a) Kong, D.; Martell, A. E.; Reibenspies, J. *Inorg. Chim. Acta* **2002**, *333*, 7. (b) Thirumavalavan, M.; Akilan, P.; Kandaswamy, M.; Chinnakali, K.; Senthil Kumar, G. *Inorg. Chem.* **2003**, *42*, 3308. (c) Fife, T.; Przystas, T. J. *J. Am. Chem. Soc.* **1985**, *107*, 1041. (d) Thirumavalavan, M.; Akilan, P.; Kandaswamy, M. *Polyhedron* **2005**, *24*, 1781. (e) Sengottuvelan, N.; Saravanakumar, D.; Kandaswamy, M. *Polyhedron* **2007**, *26*, 3825. (f) Yang, C. T.; Vetrichelvan, M.; Yang, X.; Moubaraki, B.; Murray, K. S.; Vittal, J. J. *Dalton Trans.* **2004**, 113.
(27) (a) Phillips, T.; Haq, I.; Meijer, A. J. H. M.; Adams, H.; Soutar, I.; Swanson, L.; Sykes, M. J.; Thomas, J. A. *Biochemistry* **2004**, *43*, 13657. (b) Vichard, C.; Kaden, T. A. *Inorg. Chim. Acta* **2002**, *337*, 173. (c) Zhu, L.; Santos, O.; Koo, C. W.; Rybstein, M.; Pape, L.; Canary, J. W. *Inorg. Chem.* **2003**, *42*, 7912. (d) Penkova, L. V.; Macia-g, A.; Rybak-Akimova, E. V.; Haukka, M.; Pavlenko, V. A.; Iskenderov, T. S.; Kozzowski, H.; Meyer, F.; Fritsky, I. O. *Inorg. Chem.* **2009**, *48*, 6960. (e) Iranzo, O.; Kovalevsky, A. Y.; Morrow, J. R.; Richard, J. P. *J. Am. Chem. Soc.* **2003**, *125*, 1988.
(28) Akine, S.; Taniguchi, T.; Nabeshima, T. *Inorg. Chem.* **2004**, *43*, 6142.
(29) Angeles-Boza, A. M.; Bradley, P. M.; Fu, P. K.-L; Wicke, S. E.; Bacsa, J.; Dunbar, K. R.; Turro, C. *Inorg. Chem.* **2004**, *43*, 8510.
(30) He, J.; Sun, J.; Mao, Z.-W.; Ji, L.-N.; Sun, H. *J. Inorg. Biochem.* **2009**, *103*, 851.
(31) Ivanov, V. I.; Minchenkova, L. E.A.; Schyolkina, K.; Poletayer, A. I. *Biopolymers* **1973**, *12*, 89.
(32) Uma, V.; Kanthimathi, M.; Weyhermuller, T.; Unni Nair, B. *J. Inorg. Biochem.* **2005**, *99*, 2299.

(33) Veal, J. M.; Rill, R. L. *Biochemistry* **1991**, *30*, 1132.
(34) Tan, J.; Wang, B.; Zhu, L. *Bioorg. Med. Chem. Lett.* **2007**, *17*, 1197.
(35) Young, M. J.; Chin, J. *J. Am. Chem. Soc.* **1995**, *117*, 10577.
(36) (a) Fry, F. H.; Moubaraki, B.; Murray, K. S.; Spiccia, L.; Warren, M.; Skelton, B. W.; White, A. H. *Dalton Trans.* **2003**, 866. (b) Feng, G.; Mareque-Rivas, J. C.; Williams, N. H. *Chem. Commun.* **2006**, 1845. (c) Qian, J.; Gu, W.; Liu, H.; Gao, F.; Feng, L.; Yan, S.; Liao, D.; Cheng, P. *Dalton Trans.* **2007**, 1060. (d) El Ghachtouli, S.; Cadiou, C.; Déchamps-Olivier, I.; Chuburu, F.; Aplincourt, M.; Turcry, V.; Le Baccon, M.; Handel, H. *Eur. J. Inorg. Chem.* **2005**, 2658. (e) Bazzicalupi, C.; Bencini, A.; Faggi, E.; Garau, A.; Giorgi, C.; Lippolis, V.; Perra, A.; Valtancoli, B. *Dalton Trans.* **2006**, 1409.
(37) Humphry, T.; Forconi, M.; Williams, N. H.; Hengge, A. C. *J. Am. Chem. Soc.* **2002**, *124*, 14860.
(38) (a) Sreedhara, A.; Freed, J. D.; Cowan, J. A. *J. Am. Chem. Soc.* **2000**, *122*, 8814. (b) Wright, D. J.; Jack, W. E.; Modrich, P. *J. Biol. Chem.* **1999**, *274*, 31896. (c) Stanford, N. P.; Halford, S. E.; Baldwin, G. S. *J. Mol. Biol.* **1999**, *288*, 105.
(39) Qian, J.; Wang, L.; Gu, W.; Liu, X.; Tian, J.; Yan, S. *Dalton Trans.* **2011**, *40*, 5617.
(40) Williams, N. H.; Chin, J. *Chem. Commun.* **1996**, 131.
(41) Sreedhara, A.; Cowan, J. A. *J. Biol. Inorg. Chem.* **2001**, *6*, 337.
(42) Rey, N. A.; Neves, A.; Silva, P. P.; Paula, F. C. S.; Silveira, J. N.; Botelho, F. V.; Vieira, L. Q.; Pich, C. T.; Terenzi, H.; Pereira-Maia, E. C. *J. Inorg. Biochem.* **2009**, *103*, 1323.
(43) Liang, F.; Wu, C.; Lin, H.; Li, T.; Gao, D.; Li, Z.; Wei, J.; Zheng, C.; Sun, M. *Bioorg. Med. Chem. Lett.* **2003**, *13*, 2469.
(44) (a) Sbovata, S. M.; Bettio, F.; Mozzon, M.; Bertani, R.; Venzo, A.; Benetollo, F.; Michelin, R. A.; Gandin, V.; Marzano, C. *J. Med. Chem.* **2007**, *50*, 4775. (b) Chen, T.; Liu, Y.; Zheng, W.-J.; Liu, J.; Wong, Y.-S. *Inorg. Chem.* **2010**, *49*, 6366.
(45) Sihn, C. R.; Suh, E. J.; Lee, K. H.; Kim, T. Y.; Kim, S. H. *Cancer Lett.* **2003**, *201*, 203.
(46) (a) Heffeter, P.; Jakupec, M. A.; Korner, W.; Wild, S.; Von Keyserlingk, N. G.; Elbling, L.; Zorbas, H.; Koryneuska, A.; Knasmuller, S.; Sutterluty, H.; Micksche, M.; Keppler, B. K.; Berger, W. *Biochem. Pharmacol.* **2006**, *71*, 426. (b) Sprenger, C. C.; Vail, M. E.; Simurdak, J.; Plymate, S. R. *Oncogene* **2000**, *21*, 140. (c) Wang, T.-C.; Chen, L.-L.; Lu, P.-J.; Wong, C.-H.; Liao, C.-H.; Tsiao, K.-C.; Chang, K.-M.; Chen, Y.-L.; Tzeng, C.-C. *Bioorg. Med. Chem.* **2005**, *13*, 6045.
(47) Singh, N. P.; McCoy, M. T.; Tice, R. R.; Schneider, E. L. *Exp. Cell Res.* **1988**, *175*, 184.
(48) (a) Zhang, M. C.; Liu, H. P.; Demchik, L. L.; Zhai, Y. F.; Yang, D. J. *Cell Res.* **2004**, *14*, 117. (b) Hsu, H. F.; Houng, J. Y.; Kuo, C. F.; Tsao, N.; Wu, Y. C. *Food Chem. Toxicol.* **2008**, *46*, 3785.
(49) Kim, B. S.; Yoon, K. H.; Oh, H. M.; Choi, E. Y.; Kim, S. W.; Han, W. C.; Kim, E. A.; Choi, S. C.; Kim, T. H.; Yun, K. J.; Kim, E. C.; Lyou, J. H.; Nah, Y. H.; Chung, H. T.; Cha, Y. N.; Jun, C. D. *Cell Immunol.* **2002**, *220*, 96.
(50) Murray, R. K.; Granner, D. K.; Mayes, P. A.; Rodwell, V. W. *Harper's Illustrated Biochemistry*; Lange Medical Books/McGraw-Hill: New Delhi, 2003.